Sensitivity of time lapse seismic data to the compliance of hydraulic fractures

Xinding Fang[*], Xuefeng Shang, and Michael Fehler, Massachusetts Institute of Technology, Cambridge, MA

Summary

We study the sensitivity of seismic waves to changes in the fracture normal and tangential compliances by analyzing the fracture sensitivity wave equation, which is derived by differentiating the elastic wave equation with respect to the fracture compliance. The sources for the sensitivity wavefield are the sensitivity moments, which are functions of fracture compliance, background elastic properties and the stress acting on the fracture surface. Based on the analysis of the fracture sensitivity wave equation, we give the condition for the weak scattering approximation to be valid for fracture scattering. Under the weak scattering approximation, we find that the percentage change of fracture compliance in hydraulic fracturing is equal to the percentage change of the recorded time-lapse seismic data. This could provide a means for monitoring the opening/closing of fractures in hydraulic fracturing through time-lapse seismic surveys.

Introduction

For low permeability reservoirs such as tight shale gas, hydraulic fracturing is frequently conducted to develop more connected fracture networks to enhance oil and gas recovery (King, 2010). Currently, microseismic monitoring of hydraulic fracturing is the primary method for characterizing the fracturing process (Fisher et al., 2004; Song and Toksöz, 2011). However, this method can only reveal the locations where rocks break or where existing faults are reactivated (Willis et al., 2012), and microseismicity may not have a direct relation to changes in reservoir properties during fluid injection. Recent studies have shown that scattered (diffracted) waves from fractures in a reservoir can be detected and characterized from either surface seismic data (Willis et al., 2006; Fang et al., 2012; Zheng et al., 2012) or vertical seismic profile (VSP) data (Willis et al., 2007; Willis et al., 2008; Willis et al., 2012). Field experiments have also demonstrated that the strength of fracture scattered waves can change notably during hydraulic fracturing, and such changes are attributed to the opening or closing of fluid induced fractures (Dubos-Sallée and Rasolofosaon, 2008; Willis et al., 2012).

Time-lapse seismic surveys play an important role in the evaluation of elastic parameter changes during hydrocarbon production and in monitoring fluid migration after carbon sequestration (e.g. Arts et al., 2004; Calvert, 2005; Shang and Huang, 2012). Time-lapse surveys consist of the collection of two or more seismic acquisitions recorded by the same source-receiver configuration but at different times. The changes in elastic properties between surveys can then be determined using an inversion method. Denli and Huang (2010) introduced the elastic wave sensitivity equation for time-lapse monitoring study, which quantifies the seismic sensitivity with respect to the change of some physical parameter for a given monitoring target.

The elastic properties of fractures can be described by a compliance matrix (Schoenberg, 1980). Previous studies have mainly focused on characteristics of scattering from fractures as a means of fracture characterization (e.g. Chen et al., 2012; Fang et al., 2013). In this paper, we propose an analysis of the sensitivity of time-lapse seismic data to the fracture compliance.

Linear slip fracture model

We use the linear slip model proposed by Schoenberg (1980). In this model, a fracture is represented as an imperfectly bonded interface between two elastic media. Traction is continuous across the fracture, while displacement is discontinuous. The displacement discontinuity across the fracture is given by

$$\Delta u_i = Z_{ij}\sigma_{jk}n_k \tag{1}$$

where Δu_i is the i-th component of the displacement discontinuity, σ_{jk} is the stress tensor, Z_{ij} is the fracture compliance matrix, n_k is the fracture normal.

For a rotationally invariant planar fracture, the fracture compliance matrix Z only contains two independent components: normal compliance Z_N and tangential compliance Z_T (Schoenberg, 1980). For a single planar fracture in an isotropic background, the medium in the vicinity of the fracture can be considered to be transversely isotropic with the symmetry axis perpendicular to the fracture. The effective stiffness tensor of the medium can be explicitly expressed as a function of fracture compliance and background elastic properties (Schoenberg and Sayers, 1995).

Fracture sensitivity wave equation

Denli and Huang (2010) developed an elastic wave sensitivity analysis approach for designing optimal seismic monitoring surveys. They studied the sensitivity of the seismic wave field to the reservoir properties by numerically solving a sensitivity wave equation, which is obtained by differentiating the elastic wave equation with respect to geophysical parameters. We follow their idea to study the sensitivity of seismic waves to the fracture compliance. The sensitivity wave equation for fracture

compliance is obtained by differentiating the elastic wave equation with respect to the fracture compliance (Z_N, Z_T),

$$\begin{cases} \rho \dfrac{\partial^2}{\partial t^2}\left(\dfrac{\partial u_i}{\partial Z_\xi}\right) = \dfrac{\partial}{\partial x_j}\left(\dfrac{\partial \sigma_{ij}}{\partial Z_\xi}\right) \\[2ex] \dfrac{\partial \sigma_{ij}}{\partial Z_\xi} = C_{ijkl}\dfrac{\partial}{\partial x_l}\left(\dfrac{\partial u_k}{\partial Z_\xi}\right) - M_{ij} \end{cases} \tag{2}$$

with

$$M_{ij} = -\frac{\partial C_{ijkl}}{\partial Z_\xi}\frac{\partial u_k}{\partial x_l} \tag{3}$$

where $\partial u_i/\partial Z_\xi$ represents the sensitivity of displacement to fracture compliance Z_ξ ($\xi = N$, T), M_{ij} is defined as the sensitivity moment which is a function of fracture compliance and strain at the fracture surface, C_{ijkl} is the effective stiffness tensor of the medium containing a planar fracture.

Equation 2 is analogous to a wave equation for $\partial u_i/\partial Z_\xi$. The source for the wave equation is the term M_{ij}, which has non-zero values only on the fracture plane and must be determined by solving first the elastic wave equation to obtain $\partial u_k/\partial x_l$. Hereafter, seismic wave field and sensitivity field refer to u_i and $\partial u_i/\partial Z_\xi$, respectively.

Using the effective stiffness tensor C_{ijkl} given by Schoenberg and Sayers (1995) and assuming that the fracture symmetry axis is parallel to the x_1 direction, after some algebraic manipulation, we have

$$M^N = A_N \begin{bmatrix} \sigma_{11} & 0 & 0 \\ 0 & \gamma\sigma_{11} & 0 \\ 0 & 0 & \gamma\sigma_{11} \end{bmatrix} \tag{4}$$

$$M^T = A_T \begin{bmatrix} 0 & \sigma_{12} & \sigma_{13} \\ \sigma_{12} & 0 & 0 \\ \sigma_{13} & 0 & 0 \end{bmatrix} \tag{5}$$

with

$$A_\xi = \frac{1}{Z_\xi + \eta_\xi} \tag{6}$$

where η_ξ is the matrix compliance and it is equal to $1/(\lambda+2\mu)$ for $\xi=N$ and $1/\mu$ for $\xi=T$, λ and μ are the Lame moduli of background medium, $\gamma = \lambda/(\lambda+2\mu)$, the superscripts '$N$' and '$T$' indicate the sensitivity moments for normal and tangential compliance sensitivity, respectively.

For fracture normal compliance, the strength of the sensitivity field is proportional to A_N and the normal stress resolved on the fracture plane, while its pattern is controlled by the parameter γ which is a function of background medium elastic moduli. For fracture tangential compliance, the strength of the sensitivity field is proportional to A_T and the shear stresses acting on the

fracture plane, and its pattern is controlled by the ratio of the two shear stresses.

Relation between time lapse seismic data and fracture compliance

If we assume σ_{11}, σ_{12} and σ_{13} have similar values, the strength of the sensitivity field $\partial u_i/\partial Z_\xi$ is proportional to A_ξ. For weak scattering that satisfies $Z_\xi \ll \eta_\xi$, we expand A_ξ in a Taylor series,

$$A_\xi \approx \eta_\xi^{-1} \tag{7}$$

Equation 7 indicates that the amplitude of the sensitivity field is independent of fracture compliance for weak scattering given that the presence of fracture has negligible effect on the stress field. Figure 1 shows the variations of A_N (black solid curve) and A_T (black dashed curve) with fracture compliances varying from 10^{-14} m/Pa to 10^{-9} m/Pa for sandstone, carbonate, shale and granite, respectively, which are typical reservoir rocks for oil, gas or geothermal fields. The properties of these four types of rock are listed in Table 1. Both A_N and A_T are independent of fracture compliance when compliance is smaller than about 10^{-12} m/Pa for the four types of rock, while A_N and A_T decrease significantly when normal and tangential compliances exceed η_N and η_T, respectively, which are illustrated using dashed blue and red lines ,respectively, in each panel.

Table 1. Properties of four types of rock.

Rock type	V_P (m/s)	V_S (m/s)	ρ (kg/m³)
Sandstone (Mavko *et al.,* 2003)	4090	2410	2370
Carbonate (Mavko *et al.,* 2003)	5390	2970	2590
Muderong shale (Dewhurst & Siggins, 2006)	3090	1660	2200
Chelmsford granite (Lo *et al.,* 1986)	5580	3430	2610

For a flat planar fracture, the relation between fracture aperture, which is assumed to be much smaller than the seismic wave length, and fracture compliance is given as (Schoenberg, 1980)

$$Z_\xi \approx h\eta_\xi' \tag{8}$$

where η'_ξ is the compliance of fracture infill and it is equal to $1/(\lambda'+2\mu')$ for $\xi=N$ and $1/\mu'$ for $\xi=T$, λ' and μ' are the Lame moduli of the fracture infilling material, h is fracture aperture.

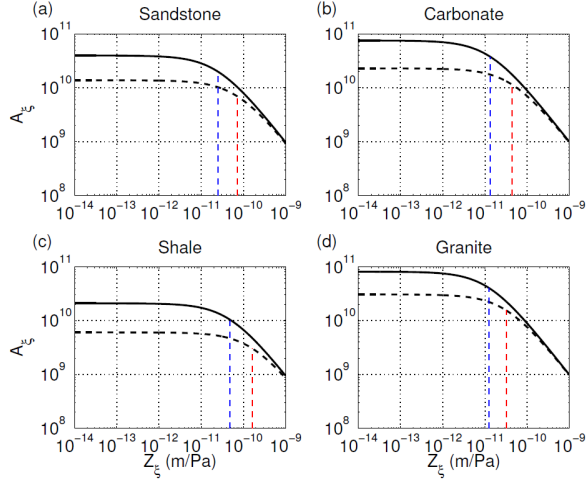# Seismic sensitivity in hydraulic fracturing

Figure 1: (a), (b), (c) and (d) Variations of A_N (black solid curve) and A_T (black dashed curve) for sandstone, carbonate, shale and granite, respectively, with fracture compliance Z_ξ ($\xi=N,T$) varying from 10^{-14} m/Pa to 10^{-9} m/Pa. In each panel, blue and red dashed lines indicate the values of η_N and η_T, respectively. Properties of the four types of rock are listed in Table 1. Both horizontal and vertical axes are in log scale.

In hydraulic fracturing, fracture aperture is on the order of 1 mm (Perkins and Kern, 1961). For a water saturated fracture with 1 mm aperture, its normal compliance can be estimated as 4.4×10^{-13} m/Pa using equation 8. The normal compliance increases with fracture aperture and reaches 4.4×10^{-12} m/Pa for a 10 mm wide fracture. The tangential compliance estimated from equation 8 goes to infinity because μ' of water is zero. This is unrealistic. The tangential compliance of a realistic fracture has a finite value due to the existence of asperities on the fracture surfaces, which are not considered in the flat planar fracture model. The tangential compliance of a realistic fracture is found to be larger than its normal compliance and it can be one order of magnitude larger than the normal compliance for a fluid saturated fracture (Lubbe et al., 2008). If we consider a fracture with aperture no larger than 10 mm, then both its normal and tangential compliances fall in the weak scattering regime for typical reservoir rocks, as shown in Figure 1. Therefore, the weak scattering assumption is valid for the study of scattering from fractures in hydraulic fracturing.

Assuming that the presence of a fracture has negligible effect on the stress field, then the strength of the fracture scattered waves is mainly affected by A_ξ in equations 4 and 5. By integrating A_ξ with respect to Z_ξ, we have

$$\vec{u} \propto \ln\left(1+\frac{Z_\xi}{\eta_\xi}\right) \qquad (9)$$

For weak scattering that has $Z_\xi \ll \eta_\xi$, equation 9 can be simplified as

$$\vec{u} \propto Z_\xi \qquad (10)$$

Equation 10 indicates that the strength of fracture scattered waves is linearly proportional to the fracture compliance for weak scattering. Fang et al. (2013) found the same linear relationship between fracture scattering strength and fracture compliance when compliance is less than 10^{-10} m/Pa, and they argued that the departure of this linear relationship at large compliance is due to the breakdown of the Born approximation. We here demonstrate that $Z_\xi \ll \eta_\xi$ is the necessary condition for the Born approximation (or weak scattering) to be valid for scattering from fractures. If the weak scattering condition is not satisfied, the relation between fracture scattering strength and fracture compliance deviates from the linear relationship (equation 10) by following a logarithmic variation (equation 9).

From equation 10, we can obtain the relation between the change of time lapse wave field and the change of fracture compliance in hydraulic fracturing as

$$\frac{\Delta\vec{u}}{\vec{u}_{base}} = \frac{\vec{u}_{lapse} - \vec{u}_{base}}{\vec{u}_{base}} \approx \frac{\Delta Z_\xi}{Z_\xi^{base}} \qquad (11)$$

where $\vec{u}_{base}$ and $\vec{u}_{lapse}$ represent the baseline and time lapse wavefields, respectively, $\Delta\vec{u}$ is the change between the two time lapse wavefields, Z_ξ^{base} is the fracture compliance before fracturing and ΔZ_ξ represents the change of fracture compliance in hydraulic fracturing.

Equation 11 indicates that the percentage change of time lapse data is equal to the percentage change of fracture compliance in hydraulic fracturing for weak scattering. Based on equation 11 and an appropriate rock physics model, we may be able to obtain information about fracture opening in hydraulic fracturing based on the percentage change of time lapse seismic data since fracture compliance is a function of fracture aperture.

As compliance becomes larger, the amplitude of the scattered wavefield increases. However, when scattering becomes strong, the breakdown of the Born approximation means that the sensitivity of the scattered wavefiled, *i.e.* the proportional change of the scattered wavefield with change in compliance, decreases.

Relative strength of normal and tangential compliance sensitivities

Assuming σ_{11}, σ_{12} and σ_{13} in equations 4 and 5 have similar values, the relative strength of M^N and M^T is similar to

Seismic sensitivity in hydraulic fracturing

$$\frac{A_N}{A_T} = \frac{\lambda + 2\mu + \mu(\lambda + 2\mu)Z_T}{\mu + \mu(\lambda + 2\mu)Z_N} \qquad (12)$$

The relative magnitudes of A_N and A_T depend on the values of Z_N and Z_T. The Z_N/Z_T ratio is strongly influenced by the way the fracture surfaces interact and it can be taken as an indicator representing the fracture saturation condition (Dubos-Sallée and Rasolofosaon, 2008; Fang et al., 2013). Both numerical simulations (Sayers et al., 2009; Gurevich et al., 2009) and laboratory measurements (Lubbe et al., 2008; Gurevich et al., 2009) suggest that Z_N is generally smaller than Z_T for reservoir fractures. Based on laboratory experimental data, Lubbe et al. (2008) pointed that the Z_N/Z_T ratio is close to 0.5 for gas-filled fractures, and Z_N/Z_T can be less than 0.1 for fluid-saturated fractures. Figures 2a, b and c, respectively, show the variations of A_N/A_T with Z_N for Z_N/Z_T=0.5, which represents a gas-filled fracture, and Z_N/Z_T=0.1 and 0.05, which represent fluid-saturated fractures. A_N/A_T is larger than 1 regardless of the compliance value and fracture saturation condition and its value increases with decreasing Z_N/Z_T ratio. Also, the normal stress σ_{11} is generally larger than the shear stresses σ_{12} and σ_{13} since P-wave source is commonly used in exploration. Therefore, the sensitivity of seismic surveys to fracture normal compliance is always larger than that to the tangential compliance.

Conclusions

Under the weak scattering approximation, which we have shown is valid for a range of fracture compliance values of relevance to subsurface conditions, we have demonstrated that the percentage change of time lapse seismic data is equal to the percentage change of fracture compliance in hydraulic fracturing. This could provide a means for determining fracture opening using time lapse data since fracture compliance is a function of fracture aperture. Also, we demonstrate that the sensitivity of seismic waves to fracture normal compliance is always larger than that to tangential compliance regardless of the compliance value. A further study of the characteristic of the sensitivity wavefield for specific fracture and acquisition geometries can be conducted by numerically solving the fracture sensitivity wave equation (*i.e.* equation 2).
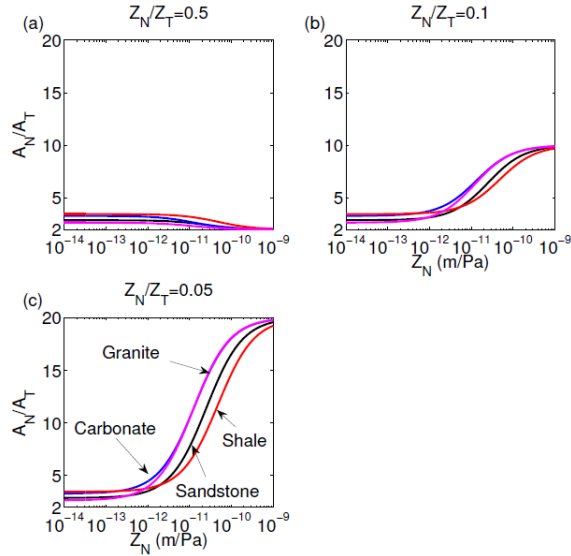
Figure 2: (a) (b) and (c) Variations of A_N/A_T (equation 12) with Z_N for Z_N/Z_T =0.5, 0.1 and 0.05, respectively. Black, blue, red and magenta curves show the variations for sandstone, carbonate, shale and granite, respectively. The properties of rocks are listed in Table 1. Horizontal axes are in log scale. Vertical axes are in linear scale.

Seismic sensitivity in hydraulic fracturing

References

Arts, R., O. Eiken, A. Chadwick, P. Zweigel, L. Van der Meer, and B. Zinszner, 2004, Monitoring of CO2 injected at Sleipner using time-lapse seismic data: Energy, **29**, 1383–1392.

Calvert, R., 2005, Insights and methods for 4D reservoir monitoring and characterization: EAGE/SEG Distinguished Instructor Short Course 8.

Chen, T.R., M. Fehler, X.D. Fang, X.F. Shang, and D. Burns, 2012, SH wave scattering from 2-D fractures using boundary element method with linear slip boundary condition: Geophys. J. Int., **188**, 371-380.

Denli, H., and L. Huang, 2010, Elastic-wave sensitivity propagation: Geophysics, **75**, T83-T97.

Dewhurst, D.N., and A.F. Siggins, 2006, Impact of fabric, microcracks and stress field on shale anisotropy: Geophys. J. Int., **165**, 135-148.

Dubos-Sallée, N., and P. Rasolofosaon, 2008, Evaluation of fracture parameters and fluid content from seismic and well data: SEG Technical Program Expanded Abstracts 2008.

Fang, X.D., M. Fehler, T.R. Chen, D. Burns, and Z.Y. Zhu, 2013, Sensitivity analysis of fracture scattering: Geophysics, **78**, T1-T10.

Fang, X.D., M. Fehler, Z.Y. Zhu, Y.C. Zheng, and D. Burns, 2012, Reservoir fracture characterizations from seismic scattered waves: SEG Technical Program Expanded Abstracts 2012.

Fisher, M.K., J.R. Heinze, C.D. Harris, B.M. Davidson, C.A. Wright, and K.P. Dunn, 2004, Optimizing horizontal completion techniques in the Barnet Shale using microseismic fracture mapping: SPE Annual Technical Conference and Exhibition.

Gurevich, B., D. Makarynska, and M. Pervukhina, 2009, Are penny-shaped cracks a good model for compliant porosity?: SEG Technical Program Expanded Abstracts 2009.

King, G.E., 2010, Thirty years of gas shale fracturing: what have we learned?: SPE Annual Technical Conference and Exhibition.

Lo, T., K.B. Coyner, and M.N. Toksöz, 1986, Experimental determination of elastic anisotropy of Berea sandstone, Chicopee shale, and Chelmsford granite: Geophysics, **51**, 164-171.

Lubbe, R., J. Sothcott, M.H. Worthington, and C. McCann, 2008, Laboratory estimates of normal and shear fracture compliance: Geophysical Prospecting, **56**, 239-247.

Mavko, Gary, T. Mukerji, J. Dvorkin, 2003, The rock physics handbook: tools for seismic analysis in porous media: Cambridge University Press.

Perkins, T.K., and L.R. Kern, 1961, Widths of hydraulic fractures: Journal of Petroleum Technology, **13**(9), 937-949.

Sayers, C.M., A.D. Taleghani, and J. Adachi, 2009, The effect of mineralization on the ratio of normal to tangential compliance of fractures: Geophysical Prospecting, **57**, 439-446.

Schoenberg, M., 1980, Elastic wave behavior across linear slip interfaces: J. Acoust. Soc. Am., **68**, 1516-1521.

Schoenberg, M., and C.M. Sayers, 1995, Seismic anisotropy of fractured rock: Geophysics, **60**, 204-211.

Shang, X., and L. Huang, 2012, Optimal designs of time-lapse seismic surveys for monitoring CO2 leakage through fault zones: International Journal of Greenhouse Gas Control, **10**, 419-433.

Song, F., and M.N. Toksöz, 2011, Full-waveform based complete moment tensor inversion and source parameter estimation from downhole microseismic data for hydrofracture monitoring: Geophysics, **76**, WC101-WC114.

Willis, M.E., D. Burns, R. Lu, M.N. Toksöz, and N. House, 2007, Fracture quality from integrating time-lapse VSP and microseismic data: The Leading Edge, **26**(9), 1198-1202.

Wiilis, M.E., D. Burns, R. Rao, B. Minsley, M.N. Toksöz, and L. Vetri, 2006, Spatial orientation and distribution of reservoir fractures from scattered seismic energy: Geophysics, **71**(5), O43-O51.

Wiilis, M.E., D. Burns, K. Willis, N. House, and J. Shemeta, 2008, Hydraulic fracture quality from time lapse VSP and microseismic data: SEG Technical Program Expanded Abstracts 2008.

Willis, M.E., X.D. Fang, D. Pei, X.F. Shang, and C.H. Cheng, 2012, Advancing the use of rapid time lapse shear wave VSPs for capturing diffractions to find hydraulic fracture dimensions: 74th EAGE Conference & Exhibition, EAGE, Expanded Abstract.

Zheng, Y.C., X.D. Fang, M. Fehler, and D. Burns, 2012, Seismic characterization of fractured reservoirs using 3D double beams: SEG Technical Program Expanded Abstracts 2012.